Vol 453|1 May 2008|doi:10.1038/nature06866

LETTERS

BCR–ABL1 lymphoblastic leukaemia is characterized by the deletion of Ikaros

Charles G. Mullighan[1], Christopher B. Miller[1], Ina Radtke[1], Letha A. Phillips[1], James Dalton[1], Jing Ma[4], Deborah White[5], Timothy P. Hughes[5], Michelle M. Le Beau[6], Ching-Hon Pui[2], Mary V. Relling[3], Sheila A. Shurtleff[1] & James R. Downing[1]

The Philadelphia chromosome, a chromosomal abnormality that encodes BCR–ABL1, is the defining lesion of chronic myelogenous leukaemia (CML) and a subset of acute lymphoblastic leukaemia (ALL)[1–3]. To define oncogenic lesions that cooperate with BCR–ABL1 to induce ALL, we performed a genome-wide analysis of diagnostic leukaemia samples from 304 individuals with ALL, including 43 *BCR–ABL1* B-progenitor ALLs and 23 CML cases. *IKZF1* (encoding the transcription factor Ikaros) was deleted in 83.7% of *BCR–ABL1* ALL, but not in chronic-phase CML. Deletion of *IKZF1* was also identified as an acquired lesion at the time of transformation of CML to ALL (lymphoid blast crisis). The *IKZF1* deletions resulted in haploinsufficiency, expression of a dominant-negative Ikaros isoform, or the complete loss of Ikaros expression. Sequencing of *IKZF1* deletion breakpoints suggested that aberrant RAG-mediated recombination is responsible for the deletions. These findings suggest that genetic lesions resulting in the loss of Ikaros function are an important event in the development of *BCR–ABL1* ALL.

Acute lymphoblastic leukaemia (ALL) comprises a heterogeneous group of disorders characterized by recurring chromosomal abnormalities including translocations, trisomies and deletions. An ALL subtype with especially poor prognosis is characterized by the presence of the Philadelphia chromosome arising from the t(9;22)(q34;q11.2) translocation, which encodes the constitutively activated BCR–ABL1 tyrosine kinase. *BCR–ABL1*-positive ALL constitutes 5% of paediatric B-progenitor ALL and approximately 40% of adult ALL[1,2]. Expression of BCR–ABL1 is also the pathological lesion underlying CML[3]. Data from murine studies demonstrate that expression of BCR–ABL1 in haematopoietic stem cells can alone induce a CML-like myeloproliferative disease, but cooperating oncogenic lesions are required for the generation of a blastic leukaemia[4,5]. Although the p210 and p190 *BCR–ABL1* fusions are most commonly found in CML and paediatric *BCR–ABL1* ALL, respectively, either fusion may be found in adult *BCR–ABL1* ALL[6]. Notably, a number of genetic lesions including additional cytogenetic aberrations and mutations in tumour suppressor genes have been described in CML cases progressing to blast crisis[7]. However, the specific lesions responsible for the generation of *BCR–ABL1* ALL and blastic transformation of CML remain incompletely understood[7]. To identify cooperating oncogenic lesions in ALL, we recently performed a genome-wide analysis of paediatric ALL[8]. This analysis identified an average of 6.8 genomic copy number alterations in 9 *BCR–ABL1* ALL cases, including deletions in genes that have a regulatory role in normal B-cell development.

To extend this analysis and identify lesions that distinguish CML from *BCR–ABL1* ALL, we have now examined DNA from leukaemic samples from 304 paediatric and adult cases of ALL (254 B-progenitor; 50 T-lineage), including 21 paediatric and 22 adult *BCR–ABL1* ALL cases, and 23 adult CML cases (Supplementary Table 1). Samples were analysed using the 250K Sty and Nsp Affymetrix single-nucleotide polymorphism (SNP) arrays (and also the 100K arrays for most cases). This identified a mean of 8.79 somatic copy number alterations per *BCR–ABL1* ALL case (range 1–26), with 1.44 gains (range 0–13) and 7.33 losses (range 0–25) (Supplementary Table 4). No significant differences were noted in the frequency of copy number alterations between paediatric and adult *BCR–ABL1* ALL cases. The most frequent somatic copy number alteration was deletion of *IKZF1*, which encodes the transcription factor Ikaros (Table 1). *IKZF1* was deleted in 36 (83.7%) of 43 *BCR–ABL1* ALL cases, including 76.2% of paediatric and 90.9% of adult *BCR–ABL1* ALL cases. *CDKN2A* was deleted in 53.5% of *BCR–ABL1* ALL cases, most of which (87.5%) also had deletions of *IKZF1* (Table 1 and Supplementary Table 5). Conversely, of the *BCR–ABL1* ALL cases with *IKZF1* deletions, 41.6% lacked *CDKN2A* alterations. Deletion of *PAX5* occurred in 51% of *BCR–ABL* ALL cases, again with the majority also having a deletion of *IKZF1* (95%) (Table 1 and Supplementary Table 5). No other defining copy number alterations were identified in the rare *BCR–ABL1* ALL cases that lacked a deletion of *IKZF1*.

Ikaros is a member of a family of zinc-finger nuclear proteins that is required for normal lymphoid development[9–12]. Ikaros has a central DNA-binding domain consisting of four zinc fingers, and a homo- and heterodimerization domain consisting of the two carboxy-terminal zinc fingers[13] (Fig. 1 and Supplementary Fig. 1). Alternative splicing generates multiple Ikaros isoforms, several of which lack the amino-terminal zinc fingers required for DNA binding; however, the physiological relevance of these isoforms in normal haematopoiesis remains unclear[9–11,14] (Supplementary Fig. 1). The *IKZF1* deletions identified in *BCR–ABL1* ALL were predominantly mono-allelic and were limited to the gene in 25 cases, conclusively identifying *IKZF1* as the genetic target (Fig. 1). In 19 cases the deletions were confined to a subset of internal *IKZF1* exons, most commonly exons 3–6 (Δ3–6; $N = 15$). Notably, the Δ3–6 deletion is predicted to encode an Ikaros isoform that lacks the DNA-binding domain but retains the C-terminal zinc fingers. The *IKZF1* deletions were confirmed by fluorescence *in situ* hybridization (FISH) and genomic quantitative polymerase chain reaction (PCR), and were in the predominant leukaemic clone (Supplementary Table 6 and Supplementary Fig. 2). Detailed analysis failed to reveal any evidence of either *IKZF1* point mutations or inactivation of its promoter by CpG methylation in primary ALL samples (data not shown and Supplementary Fig. 8).

[1]Departments of Pathology, [2]Oncology and [3]Pharmaceutical Sciences and [4]The Hartwell Center for Bioinformatics and Biotechnology, St Jude Children's Research Hospital, Memphis, Tennessee 38105, USA. [5]Division of Haematology, The Institute for Medical and Veterinary Science, Adelaide, South Australia 5000, Australia. [6]Section of Hematology/Oncology, University of Chicago, Chicago, Illinois 60637, USA.

Table 1 | Frequency of recurring DNA copy number abnormalities in ALL

ALL subtype (*N*)	*IKZF1*	*CDKN2A*	*PAX5*	*C20orf94*	*RB1*	*MEF2C*	*EBF1*	*BTG1*	*DLEU*	*FHIT*	*ETV6*
B-progenitor (254)											
BCR–ABL1 (43)	36	23	22	10	8	6	6	6	4	4	3
Childhood (21)	16	10	10	7	4	2	3	4	1	2	2
Adult (22)	20	13	12	3	4	4	3	2	3	2	1
Hypodiploid (10)	5	10	10	0	0	0	1	1	0	1	2
Other B ALLs (75)	15	25	22	4	1	0	2	5	1	3	10
High hyperdiploid (39)	2	8	4	1	3	0	0	0	5	0	3
MLL-rearranged (22)	1	4	4	0	2	0	0	0	3	0	2
TCF3–PBX1 (17)	0	6	7	0	2	0	0	0	2	0	0
ETV6–RUNX1 (48)	0	14	16	6	2	0	5	7	4	6	33
T-lineage (50)	2	36	5	1	6	1	3	0	3	0	4
Total (304)	61	126	90	22	24	7	17	19	22	14	57
P-value	6.6×10^{-27}	7.4×10^{-10}	1.4×10^{-9}	7.0×10^{-8}	1.1×10^{-6}	0.0004	0.0247	1.5×10^{-7}	2.6×10^{-6}	0.0076	9.1×10^{-15}

The prevalence of recurring genomic abnormalities in *BCR–ABL1* B-progenitor ALL identified by SNP array analysis is shown for each ALL subtype. The exact likelihood ratio *P*-value for variation in the frequency of each lesion across ALL subtypes is shown. The *DLEU* region at 13q14 incorporates the microRNA genes *MIRN16-1* and *MIRN15A*.

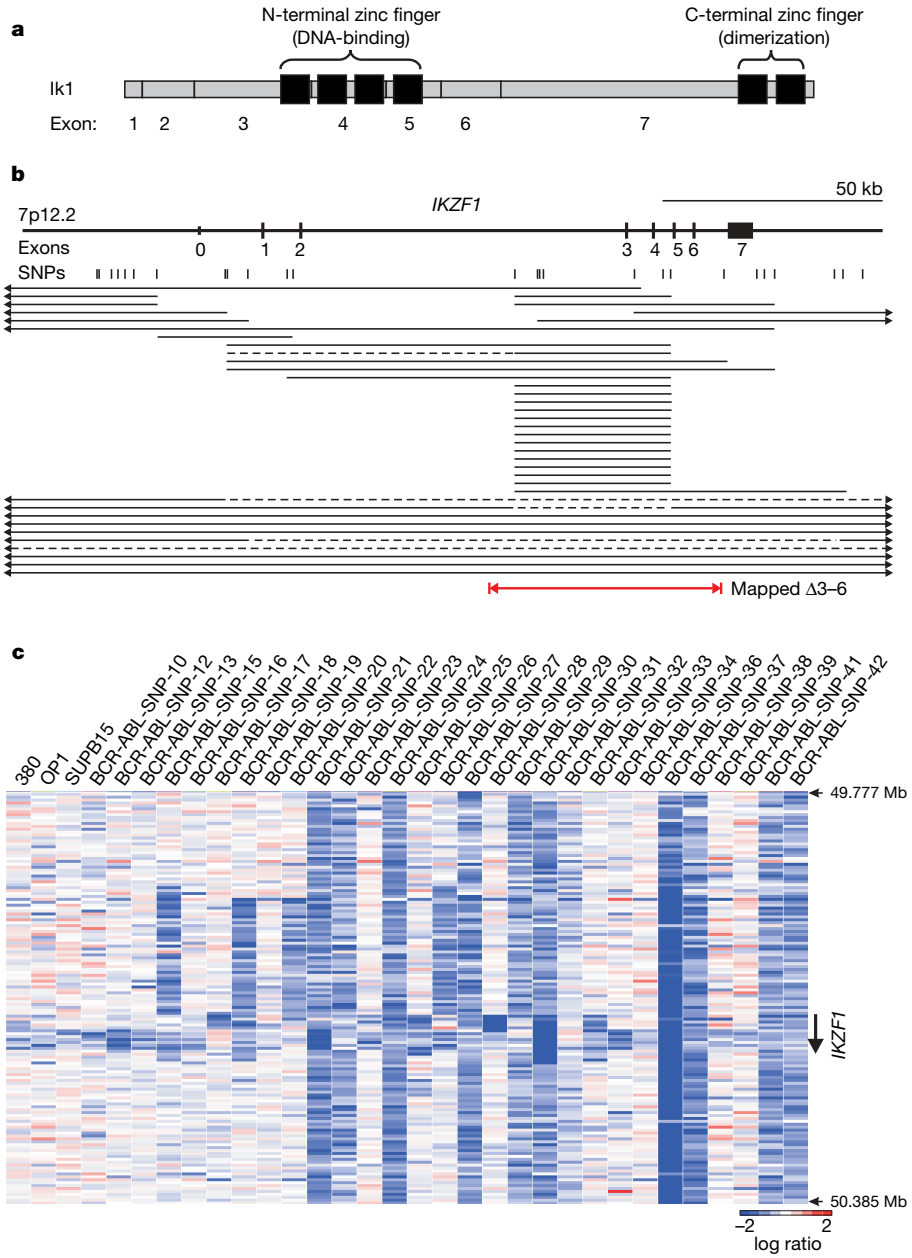

Figure 1 | *IKZF1* deletions in *BCR–ABL1* ALL. a, Domain structure of *IKZF1*. Exons 3–5 encode four N-terminal zinc fingers (black boxes) responsible for DNA binding. The C-terminal zinc fingers encoded by exon 7 are essential for homo- and heterodimerization. **b**, Genomic organization of *IKZF1* and location of each of the 36 deletions observed in *BCR–ABL1* B-progenitor ALL. Each line depicts the deletion(s) observed in each case. In four cases, two discontiguous deletions were observed. Hemizygous deletions are solid lines and homozygous deletions dashed. Arrows indicate deletions extending beyond the limits of the figure. The exact boundaries of the deletions were defined by genomic quantitative PCR, and for *IKZF1* Δ3–6, by long-range genomic PCR (red arrow). **c**, dChip SNP raw $\log_2$ ratio copy number data depicting *IKZF1* deletions for 29 *BCR–ABL1* cases and 3 B-progenitor ALL cell lines.

The expression of aberrant, dominant-negative Ikaros isoforms in B- and T-lineage ALL has been previously reported by several groups[15–22], although alternative splicing has been reported to be the underlying mechanism[23]. Importantly, the Δ3–6 isoform of Ikaros has been shown to function as a dominant-negative inhibitor of the transcriptional activity of Ikaros and related family members[13]. Moreover, mice homozygous for either an *Ikzf1* null mutation[24] or a dominant-negative *Ikzf1* mutation[25] exhibit profound defects in lymphoid development, and mice heterozygous for a dominant-negative *Ikzf1* mutation develop clonal T-cell expansions and lymphoproliferative diseases[26], demonstrating that alteration in the level of *Ikzf1* expression is oncogenic.

The high frequency of focal deletions in *IKZF1* in *BCR–ABL1* ALL suggests that expression of alternative *IKZF1* transcripts may be the result of specific genetic lesions, and not alternative splicing of an intact gene. To explore further this possibility, we performed reverse-transcriptase PCR (RT–PCR) analysis for *IKZF1* transcripts in 159 cases (Fig. 2). This demonstrated that expression of the Ik6 transcript, which lacks exons 3–6, was exclusively observed in cases harbouring the *IKZF1* Δ3–6 deletion (Fig. 2b). Furthermore, we detected two previously unknown Ikaros isoforms exclusively in cases with larger deletions: Ik9 in a case with deletion of exons 2–6, and Ik10 in three cases with deletion of exons 1–6 (Fig. 2a, b, and Supplementary Fig. 3). For each isoform, Ik6, Ik9 and Ik10, there was concordance between the transcripts detected by RT–PCR and the extent of deletion defined by SNP array and genomic PCR analysis (Fig. 2b). Moreover, analysis of 22 *IKZF1* Δ3–6 and 29 non-Δ3–6 cases with a quantitative RT–PCR assay specific for the Ik6 transcript confirmed that Ik6 expression was restricted to cases with the Δ3–6 deletion ($P = 6.41 \times 10^{-15}$, Supplementary Fig. 4). Furthermore, the Ik6 protein isoform was only detectable by western blotting in cases with a Δ3–6 *IKZF1* deletion (Fig. 2c). We also did not observe expression of Ik6 after the enforced expression of *BCR–ABL1* in *Arf* null or wild-type murine haematopoietic precursors (data not shown). Together, these data indicate that the expression of non-DNA-binding Ikaros isoforms is due to *IKZF1* genomic abnormalities, and not aberrant post-transcriptional splicing induced by BCR–ABL1, as has been suggested[23].

To identify copy number alterations in CML, we performed SNP array analysis on 23 CML cases. In addition to chronic-phase CML (CP-CML), we also examined matched accelerated phase (AP-CML, $N = 7$) and blast crisis (BC-CML, $N = 15$ (12 myeloid and 3 lymphoid)) samples (Supplementary Table 2). This identified only 0.47 copy number alterations per CP-CML case (range 0–8) (Supplementary Table 7), suggesting that *BCR–ABL1* is sufficient to induce CML, but alone does not result in substantial genomic instability. Notably, no recurrent lesions were identified. In contrast, there was a mean of 7.8 copy number alterations per BC-CML case

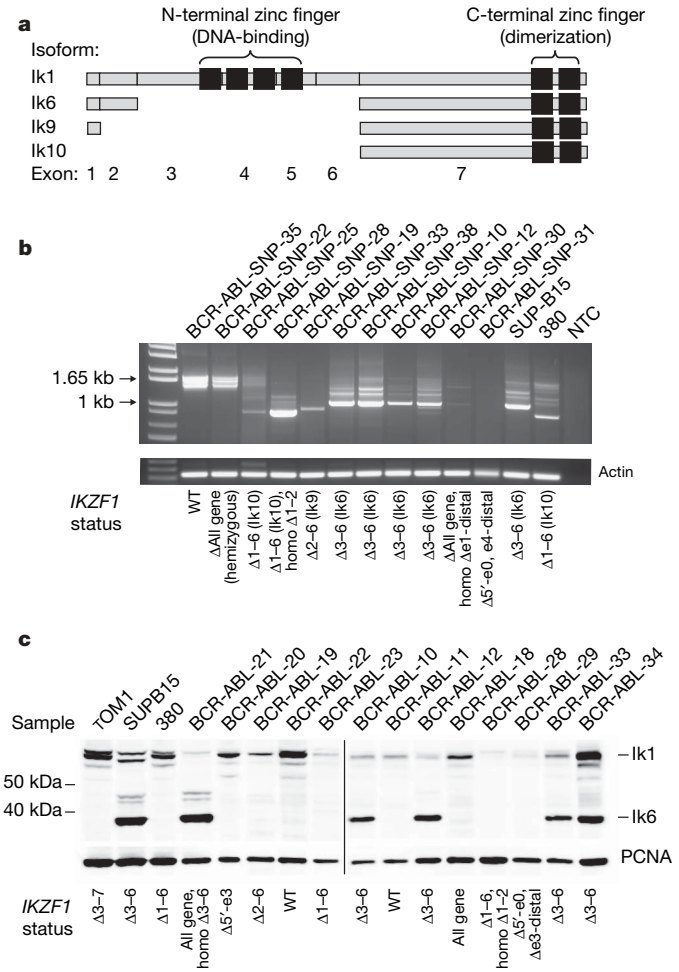

Figure 2 | Ikaros isoforms in ALL blasts. **a**, Domain structure of the *IKZF1* isoforms detected by RT–PCR, examples of which are shown in **b**. **b**, RT–PCR for *IKZF1* transcripts (using exon 0- and 7-specific primers) in representative cases with various *IKZF1* genomic abnormalities. Each case expressing an aberrant isoform has a corresponding *IKZF1* genomic deletion. *IKZF1* Δ3–6 was also detected in the *BCR–ABL1* ALL cell lines SUP-B15 and OP1, and Δ1–6 in the ALL cell line 380. **c**, Western blotting for Ikaros using a C-terminus-specific polyclonal antibody. Ik6 was only detectable in cases with *IKZF1* Δ3–6. The Δ1–6 and Δ2–6 deletions do not produce a detectable protein. In three cases with multiple focal hemizygous deletions involving different regions of *IKZF1* (BCR-ABL-SNP-26, BCR-ABL-SNP-29 and BCR-ABL-SNP-31), no wild-type Ikaros was detectable by RT–PCR or western blotting, indicating that the deletions involve both copies of *IKZF1* in each case.

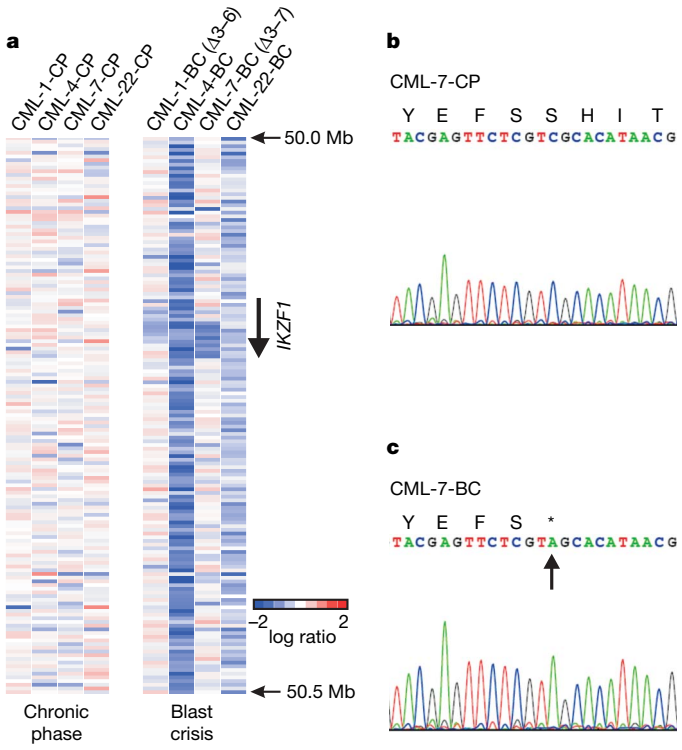

Figure 3 | *IKZF1* deletions in blast crisis CML. **a**, dChip SNP $\log_2$ ratio copy number heatmaps of four CML cases showing acquisition of *IKZF1* deletions at progression to blast crisis. **b**, **c**, Pherograms of *IKZF1* exon 7 sequencing demonstrating acquisition of the coding nucleotide 1520C>A, amino acid Ser507X mutation at chronic-phase (**b**) and blast crisis (**c**) in case CML-7. As this case has a concomitant hemizygous *IKZF1* deletion involving exon 7, the mutation appears to be homozygous.

(range 0–28) (Supplementary Table 7), with *IKZF1* deletions in four BC samples, including two of the three cases with lymphoid blast crisis (Fig. 3a). Two of the *IKZF1* deletions involved the entire gene (CML-4-BC and CML-22-BC), one Δ3–6 (CML-1-BC, which was associated with Ik6 expression by RT–PCR) and one Δ3–7 (CML-7-BC). CML-7-BC also had an *IKZF1* nonsense mutation in the C-terminal zinc-finger domain of exon 7 in the non-deleted allele (coding nucleotide 1520C>A, amino acid Ser507X, Fig. 3b, c). One BC sample had a *CDKN2A* deletion, and four cases had copy number alterations involving *PAX5* (two deletions, one internal amplification and one trisomy 9), with two of these also having *IKZF1* deletion. Copy number alterations were identified in two AP-CML samples. These data demonstrate an increased burden of genomic aberrations during progression of CML, with *IKZF1* mutation a frequent event in the transformation of CML to lymphoid blast crisis.

To explore the mechanism responsible for the identified *IKZF1* deletion, we sequenced the *IKZF1* Δ3–6 genomic breakpoints (Supplementary Fig. 6). The deletions were restricted to highly localized sequences in introns 2 and 6 (Supplementary Fig. 7). Moreover, heptamer recombination signal sequences (RSSs) recognized by the RAG enzymes during V(D)J recombination[27] were located immediately internal to the deletion breakpoints, and a variable number of additional nucleotides were present between the consensus intron 2 and 6 sequences, suggestive of the action of terminal deoxynucleotidyl transferase (TdT). Together, these data suggest that the *IKZF1* Δ3–6 deletion arises owing to aberrant RAG-mediated recombination.

We have identified a high frequency of copy number alterations in *BCR–ABL1* ALL and BC-CML, but not in CP-CML. We observed a near obligate deletion of *IKZF1* in *BCR–ABL1* ALL, with 83.7% of paediatric and adult cases containing deletions that lead to a reduction in dose and/or the expression of an altered Ikaros isoform. By contrast, deletion of *IKZF1* was not detected in CP-CML, but was identified as an acquired lesion in two of three lymphoid BC-CML samples. These data, together with the low frequency of *IKZF1* deletions in other paediatric B-progenitor ALL cases, and the lack of focal *IKZF1* aberrations in recently reported genomic analysis of non-haematopoietic tumours[28] (Supplementary Results), suggest that alterations in Ikaros directly contribute to the pathogenesis of *BCR–ABL1* ALL. How reduced activity of Ikaros, and possibly that of other family members through the expression of dominant negative Ikaros isoforms, collaborates with *BCR–ABL1* to induce lymphoblastic leukaemia remains to be determined. Importantly, mice with attenuated Ikaros expression exhibit a partial block of B lymphoid maturation at the pro-B-cell stage[29], suggesting that Ikaros loss may contribute to the arrested B-lymphoid maturation in *BCR–ABL1* ALL. However, the high co-occurrence of *PAX5* deletions in many cases suggests that *IKZF1* deletion contributes to transformation in additional ways. The frequent co-deletion of *CDKN2A* (encoding INK4A/ARF) with *IKZF1* in *BCR–ABL1* ALL is a notable finding. This suggests that attenuated Ikaros activity may either collaborate with disruption of INK4A/ARF-mediated tumour suppression, or act through alternative uncharacterized tumour suppressor pathways in ALL. Furthermore, the identification of aberrant RAG-mediated recombination as the mechanism underlying deletions of *IKZF1* suggests that the cellular target of this transforming event is downstream of the haematopoietic stem cell. Dissecting the contribution of altered Ikaros activity to *BCR–ABL1* leukaemogenesis should not only provide valuable mechanistic insights, but will also help to determine if the presence of this genetic lesion can be used to gain a therapeutic advantage against this aggressive leukaemia.

METHODS SUMMARY

Two-hundred and eighty-two paediatric ALL cases, 22 adult *BCR–ABL1* ALL cases, 49 samples obtained from 23 adult patients with chronic myeloid leukaemia (CML) and 36 leukaemia cell lines were studied (Supplementary Tables 1 and 2). Affymetrix 250K Sty and Nsp arrays were performed on all samples. 50K Hind 240 and 50K Xba 240 arrays were performed for 252 ALL samples (Supplementary Table 1). SNP array data were analysed using dChip (http://www.dChip.org), a reference normalization algorithm, and circular binary segmentation as previously described[8]. *IKZF1* deletions were confirmed by FISH and/or genomic quantitative PCR. Expression of Ikaros transcripts was examined by qualitative and quantitative RT–PCR, and western blotting. Genomic sequencing was performed for all *IKZF1* coding exons. Methylation status of the *IKZF1* promoter CpG island was performed by MALDI-TOF mass spectrometry of bisulphite-treated leukaemic blast DNA.

Full Methods and any associated references are available in the online version of the paper at www.nature.com/nature.

Received 18 December 2007; accepted 25 February 2008.
Published online 13 April 2008.

1. Ribeiro, R. C. *et al.* Clinical and biologic hallmarks of the Philadelphia chromosome in childhood acute lymphoblastic leukemia. *Blood* **70,** 948–953 (1987).
2. Gleissner, B. *et al.* Leading prognostic relevance of the BCR-ABL translocation in adult acute B-lineage lymphoblastic leukemia: a prospective study of the German Multicenter Trial Group and confirmed polymerase chain reaction analysis. *Blood* **99,** 1536–1543 (2002).
3. Goldman, J. M. & Melo, J. V. Chronic myeloid leukemia–advances in biology and new approaches to treatment. *N. Engl. J. Med.* **349,** 1451–1464 (2003).
4. Daley, G. Q., Van Etten, R. A. & Baltimore, D. Blast crisis in a murine model of chronic myelogenous leukemia. *Proc. Natl Acad. Sci. USA* **88,** 11335–11338 (1991).
5. Williams, R. T., Roussel, M. F. & Sherr, C. J. Arf gene loss enhances oncogenicity and limits imatinib response in mouse models of Bcr-Abl-induced acute lymphoblastic leukemia. *Proc. Natl Acad. Sci. USA* **103,** 6688–6693 (2006).
6. Melo, J. V. The diversity of BCR-ABL fusion proteins and their relationship to leukemia phenotype. *Blood* **88,** 2375–2384 (1996).
7. Melo, J. V. & Barnes, D. J. Chronic myeloid leukaemia as a model of disease evolution in human cancer. *Nature Rev. Cancer* **7,** 441–453 (2007).
8. Mullighan, C. G. *et al.* Genome-wide analysis of genetic alterations in acute lymphoblastic leukaemia. *Nature* **446,** 758–764 (2007).
9. Hahm, K. *et al.* The lymphoid transcription factor LyF-1 is encoded by specific, alternatively spliced mRNAs derived from the Ikaros gene. *Mol. Cell. Biol.* **14,** 7111–7123 (1994).
10. Molnar, A. & Georgopoulos, K. The Ikaros gene encodes a family of functionally diverse zinc finger DNA-binding proteins. *Mol. Cell. Biol.* **14,** 8292–8303 (1994).
11. Molnar, A. *et al.* The Ikaros gene encodes a family of lymphocyte-restricted zinc finger DNA binding proteins, highly conserved in human and mouse. *J. Immunol.* **156,** 585–592 (1996).
12. Rebollo, A. & Schmitt, C. Ikaros, Aiolos and Helios: transcription regulators and lymphoid malignancies. *Immunol. Cell Biol.* **81,** 171–175 (2003).
13. Sun, L., Liu, A. & Georgopoulos, K. Zinc finger-mediated protein interactions modulate Ikaros activity, a molecular control of lymphocyte development. *EMBO J.* **15,** 5358–5369 (1996).
14. Klug, C. A. *et al.* Hematopoietic stem cells and lymphoid progenitors express different Ikaros isoforms, and Ikaros is localized to heterochromatin in immature lymphocytes. *Proc. Natl Acad. Sci. USA* **95,** 657–662 (1998).
15. Sun, L. *et al.* Expression of dominant-negative Ikaros isoforms in T-cell acute lymphoblastic leukemia. *Clin. Cancer Res.* **5,** 2112–2120 (1999).
16. Sun, L. *et al.* Expression of aberrantly spliced oncogenic ikaros isoforms in childhood acute lymphoblastic leukemia. *J. Clin. Oncol.* **17,** 3753–3766 (1999).
17. Sun, L. *et al.* Expression of dominant-negative and mutant isoforms of the antileukemic transcription factor Ikaros in infant acute lymphoblastic leukemia. *Proc. Natl Acad. Sci. USA* **96,** 680–685 (1999).
18. Nakase, K. *et al.* Dominant negative isoform of the Ikaros gene in patients with adult B-cell acute lymphoblastic leukemia. *Cancer Res.* **60,** 4062–4065 (2000).
19. Olivero, S. *et al.* Detection of different Ikaros isoforms in human leukaemias using real-time quantitative polymerase chain reaction. *Br. J. Haematol.* **110,** 826–830 (2000).
20. Nishii, K. *et al.* Expression of B cell-associated transcription factors in B-cell precursor acute lymphoblastic leukemia cells: association with PU.1 expression, phenotype, and immunogenotype. *Int. J. Hematol.* **71,** 372–378 (2000).
21. Takanashi, M. *et al.* Expression of the Ikaros gene family in childhood acute lymphoblastic leukaemia. *Br. J. Haematol.* **117,** 525–530 (2002).
22. Tonnelle, C. *et al.* Overexpression of dominant-negative Ikaros 6 protein is restricted to a subset of B common adult acute lymphoblastic leukemias that express high levels of the CD34 antigen. *Hematol. J.* **4,** 104–109 (2003).
23. Klein, F. *et al.* BCR-ABL1 induces aberrant splicing of IKAROS and lineage infidelity in pre-B lymphoblastic leukemia cells. *Oncogene* **25,** 1118–1124 (2006).
24. Wang, J. H. *et al.* Selective defects in the development of the fetal and adult lymphoid system in mice with an Ikaros null mutation. *Immunity* **5,** 537–549 (1996).
25. Georgopoulos, K. *et al.* The Ikaros gene is required for the development of all lymphoid lineages. *Cell* **79,** 143–156 (1994).
26. Winandy, S., Wu, P. & Georgopoulos, K. A dominant mutation in the Ikaros gene leads to rapid development of leukemia and lymphoma. *Cell* **83,** 289–299 (1995).
27. Fugmann, S. D. *et al.* The RAG proteins and V(D)J recombination: complexes, ends, and transposition. *Annu. Rev. Immunol.* **18,** 495–527 (2000).

28. Weir, B. A. *et al.* Characterizing the cancer genome in lung adenocarcinoma. *Nature* **450,** 893–898 (2007).
29. Kirstetter, P. *et al.* Ikaros is critical for B cell differentiation and function. *Eur. J. Immunol.* **32,** 720–730 (2002).

Supplementary Information is linked to the online version of the paper at www.nature.com/nature.

Acknowledgements The authors thank Z. Cai for technical help, K. Rakestraw and J. Armstrong for assistance with sequencing, R. Williams and C. Sherr for the provision of Arf null hematopoietic cells and *BCR–ABL1* retroviral vectors, O. Heidenreich for providing the SKNO-1 cell line, and D. Campana for providing the OP1 cell line. This study was supported by the American Lebanese Syrian Associated Charities of St Jude Children's Research Hospital. C.G.M. was supported by grants from the National Health and Medical Research Council (Australia), the Royal Australasian College of Physicians, and the Haematology Society of Australasia.

Author Contributions C.G.M. collected and extracted clinical samples, performed laboratory assays and analysed data. C.B.M., L.A.P., J.D. and I.R. performed laboratory assays. J.M. analysed SNP array data. D.W., T.P.H., M.M.L., C.-H.P., M.V.R. and S.A.S. collected clinical samples and data. C.G.M and J.R.D designed the study and wrote the manuscript, which was reviewed by all authors.

Author Information The primary SNP microarray data have been deposited in NCBIs Gene Expression Omnibus (GEO, http://www.ncbi.nlm.nih.gov/geo/) and are accessible through GEO Series accession numbers GSE9109–GSE9113. Reprints and permissions information is available at www.nature.com/reprints. Correspondence and requests for materials should be addressed to J.R.D. (james.downing@stjude.org).

METHODS

Patients and samples. Patients and samples comprised 282 patients with acute lymphoblastic leukaemia (ALL) treated at St Jude Children's Research Hospital, 22 adult *BCR–ABL1* ALL patients treated at the University of Chicago, and 49 samples obtained from 23 adult patients with chronic myeloid leukaemia (CML) treated at the Institute of Medical and Veterinary Science, Adelaide (Supplementary Tables 1 and 2). The CML cohort included 24 chronic phase, 7 accelerated phase and 15 blast crisis samples, and three samples obtained at complete cytogenetic response. All blast crisis samples were flow sorted to at least 90% blast purity before DNA extraction using FACSVantage s.e. (with DiVa option) flow cytometers (BD Biosciences) and fluorescein-isothiocyanate-labelled CD45, allophycocyanin-labelled CD33 and phycoerythrin-labelled CD19 and CD13 antibodies (BD Biosciences). Germline tissue was obtained by also sorting the non-blast population in seven cases. Informed consent for the use of leukaemic cells for research was obtained from patients, parents or guardians in accordance with the Declaration of Helsinki, and study approval was obtained from the SJCRH institutional review board.

Cell lines examined by SNP array. Thirty-six acute myeloid and lymphoid leukaemia cell lines were genotyped using the Affymetrix Mapping 250k Sty and Nsp arrays. These were the ALL cell lines 380 (*MYC–IGH* and *BCL2–IGH* B precursor), 697 (*TCF3–PBX1*), AT1 (*ETV6–RUNX1*), BV173 (CML in lymphoid blast crisis), CCRF-CEM (*TAL–SIL*), Jurkat (T-ALL), Kasumi-2 (*TCF3–PBX1*), MHH-CALL-2 (hyperdiploid B-precursor ALL), MHH-CALL-3 (*TCF3–PBX1*), MOLT3 (T-ALL), MOLT4 (T-ALL), NALM-6 (B-precursor ALL), OP1 (*BCR–ABL1*), Reh (*ETV6–RUNX1*), RS4;11 (*MLL–AF4*), SD1 (*BCR–ABL1*), SUP-B15 (*BCR–ABL1*), TOM-1 (*BCR–ABL1*), U-937 (*PICALM–AF10*), UOCB1 (*TCF3–HLF*), YT (NK leukaemia), and the AML cell lines CMK (FAB M7), HL-60 (FAB M2), K-562 (CML in myeloid blast crisis), Kasumi-1 (*RUNX1–RUNX1T1*), KG-1 (myelocytic leukaemia), ME-1 (*CBFB–MYH11*), ML-2 (*MLL–AF6*), M-07e (FAB M7), Mono Mac 6 (*MLL–AF9*), MV4-11 (*MLL–AF4*), NB4 (*PML–RARA*), NOMO-1 (*MLL–AF9*), PL21 (FAB M3), SKNO-1 (*RUNX1–RUNX1T1*) and THP-1 (FAB M5). Cell lines were obtained from the Deutsche Sammlung von Mikroorganismen und Zellkulturen, Braunschweig, Germany, the American Type Culture Collection, Manassas, Virginia, from local institutional repositories, or were gifts from O. Heidenreich (SKNO-1) and D. Campana (OP1). Cells were cultured in accordance with previously published recommendations[30]. The paediatric *BCR–ABL1* B-precursor ALL cell line OP1 (ref. 31) was cultured in RPMI-1640 containing 100 units ml^{-1} penicillin, 100 $\mu g\,ml^{-1}$ streptomycin, 2 mM glutamine and 10% fetal bovine serum. DNA was extracted from 5×10^6 cells obtained during log-phase growth after washing in PBS using the QIamp DNA blood mini kit (Qiagen).

SNP microarray analysis. Collection and processing of diagnostic and remission bone marrow and peripheral blood samples for Affymetrix SNP microarray analysis has been previously reported in detail[8]. Affymetrix 250K Sty and Nsp arrays were performed on all samples. 50K Hind 240 and 50K Xba 240 arrays were performed for 252 ALL samples (Supplementary Table 1). SNP array .CEL and SNP call .TXT files (generated by Affymetrix GTYPE 4.0 using the DM algorithm) have been deposited in NCBIs Gene Expression Omnibus (GEO, http://www.ncbi.nlm.nih.gov/geo/) and are accessible through GEO series accession numbers GSE9109–GSE9113. These accessions contain the following data: GSE9109, Sty and Nsp files for 304 ALL samples, and Hind and Xba files for 252 of these samples; GSE9110, Sty and Nsp files for 56 CML samples; GSE9111, Sty, Nsp, Hind and Xba files for 50 remission acute leukaemia samples used as references for copy number analysis; GSE9112, Sty and Nsp files for 36 acute leukaemia cell lines; GSE9113, a superseries containing all of the above data. The data are also available at http://www.stjuderesearch.org/data/ALL-SNP2/.

FISH. FISH for *IKZF1* deletion was performed using diagnostic bone marrow or peripheral blood leukaemic cells in Carnoy's fixative as previously described[8]. BAC clones CTD-2382L6 and CTC-791O3 (for *IKZF1*, Open Biosystems) were labelled with fluorescein isothiocyanate, and control 7q31 probes RP11-460K21 (Children's Hospital Oakland Research Institute) and CTB-133K23 (Open Biosystems) were labelled with rhodamine. At least 100 interphase nuclei were scored per case.

***IKZF1* PCR, cloning, quantitative PCR and genomic sequencing.** RNA was extracted and reverse transcribed using random hexamer primers and Superscript III (Invitrogen) as previously described[8]. *IKZF1* transcripts were amplified from cDNA using the Advantage 2 PCR enzyme (Clontech) as previously described[8] using primers that anneal in exon 0 and 7 of *IKZF1*. PCR products were purified and sequenced directly and after cloning into pGEM-T-Easy (Promega). Genomic quantitative PCR for exons 1–7 of *IKZF1*, and real-time PCR to quantify expression of Ik6, were performed as previously described[8]. All primers and probes are listed in Supplementary Table 3. Genomic sequencing of *IKZF1* exons 0–7 in all ALL and CML samples was performed as previously described[8].

Western blotting. Whole-cell lysates of $3–6 \times 10^6$ leukaemic cells were prepared and blotted as previously described[8] using N- and C-terminus-specific rabbit polyclonal Ikaros antibodies (Santa Cruz Biotechnology).

Methylation analysis. Methylation status of the *IKZF1* promoter CpG island (PCR amplicon hg17 coordinates: chromosome 7 50121508–50121714) was performed using MALDI-TOF mass spectrometry of PCR-amplified, bisulphite-modified genomic DNA extracted from leukaemic cells as previously described[8,32].

Statistical analysis. Associations between ALL subtype and *IKZF1* deletion frequency were calculated using the exact likelihood ratio test. Differences in Ik6 expression between *IKZF1* Δ3–6 and non-Δ3–6 cases were assessed using the exact Wilcoxon–Mann–Whitney test. All *P*-values reported are two-sided. Analyses were performed using StatXact v8.0.0 (Cytel).

30. Drexler, H. G. *The Leukemia-Lymphoma Cell Line Facts Book* 1st edn (Academic Press, London, 2001).
31. Manabe, A. *et al.* Interleukin-4 induces programmed cell death (apoptosis) in cases of high-risk acute lymphoblastic leukemia. *Blood* **83**, 1731–1737 (1994).
32. Ehrich, M. *et al.* Quantitative high-throughput analysis of DNA methylation patterns by base-specific cleavage and mass spectrometry. *Proc. Natl Acad. Sci. USA* **102**, 15785–15790 (2005).